

RSC Advances



This is an *Accepted Manuscript*, which has been through the Royal Society of Chemistry peer review process and has been accepted for publication.

Accepted Manuscripts are published online shortly after acceptance, before technical editing, formatting and proof reading. Using this free service, authors can make their results available to the community, in citable form, before we publish the edited article. This *Accepted Manuscript* will be replaced by the edited, formatted and paginated article as soon as this is available.

You can find more information about *Accepted Manuscripts* in the [Information for Authors](#).

Please note that technical editing may introduce minor changes to the text and/or graphics, which may alter content. The journal's standard [Terms & Conditions](#) and the [Ethical guidelines](#) still apply. In no event shall the Royal Society of Chemistry be held responsible for any errors or omissions in this *Accepted Manuscript* or any consequences arising from the use of any information it contains.

Geometrical Alignment for Improving Cell Evaluation in a Microchannel with Application on Multiple Myeloma Red Blood Cells

Chia-Hung Dylan Tsai,^{*a} Shinya Sakuma,^b Fumihito Arai,^b Tatsunori Taniguchi,^c Tomohito Ohtani,^c Yasushi Sakata^c and Makoto Kaneko^a

Received Xth XXXXXXXXXXXX 20XX, Accepted Xth XXXXXXXXXXXX 20XX

First published on the web Xth XXXXXXXXXXXX 200X

DOI: 10.1039/b000000x

A microfluidic design for evaluating red blood cell deformability with geometrical alignment mechanism is proposed. While the transit velocity of a cell passing through a constriction channel is conventionally utilized as an index of cell deformability, the flow-in angle of the cell entering the channel is found affecting the transit significantly, and would interfere with the evaluation. To suppress such kind of interference, an additional alignment channel is placed in front of the evaluation channel for aligning target cells before entering the evaluation channel. Cells are spontaneously aligned by the geometrical constraints without any additional control. The Experiments on the red blood cells from three healthy subjects and a patient with multiple myeloma are conducted. According to the experimental results, the alignment channel effectively reduce 42.7% of position distribution in average, and the negative correlation between transit velocity and cell size is increased. The correlation shows the improved size sensitivity of the proposed method. For the purpose of comparison and validating the microchannel approach, the stiffness of the subjects' red blood cells is also measured by an atomic force microscope, the current gold standard of cell stiffness measurement. The results from two approaches show the same tendency of the RBC deformability, which evidently support the validity of the proposed method on cell deformability evaluation.

1 Introduction

Red blood cell (RBC) deformability has become an important index for diseases diagnosis in recent years because the relations between RBC deformability and diseases have been found from various researches. For example, malaria-infected RBCs have been found stiffer than the ones of a healthy person.^{1,2} Sickle cell anemia not only makes RBCs stiffer but also increases cell viscosity.³ Diabetic patients are also discovered having stiffened RBCs.^{4,5} In order to perform accurate and statistically meaningful evaluation on RBC deformability, a reliable and high throughput method is needed for medical applications and related studies. This paper is for the purpose, and focuses on improving the sensitivity of RBC evaluation in a microchannel.

Figures 1(a) and (b) illustrate the idea of the conventional single-channel evaluation and proposed method, respectively. Both the evaluations are based on the transit of RBCs through

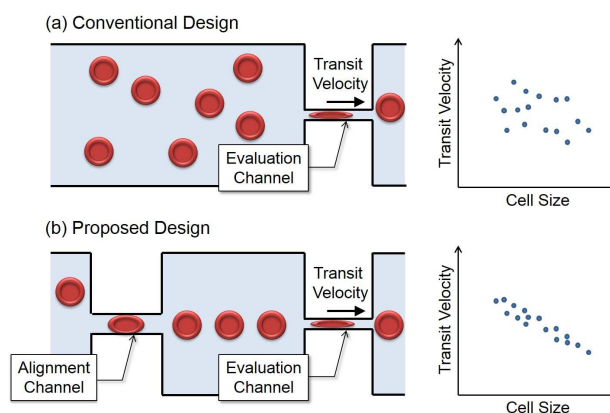


Fig. 1 (a) Evaluation without alignment (b) Evaluation with an alignment channel

the evaluation channel. The evaluation channel is generally smaller than the size of RBCs, so that the RBCs are deformed by the constriction during the transit. This kind of approach stands on the fact that the transit velocity, or transit time, of a cell through the constriction reflects the deformability of the cell. For example, a soft cell would pass through a constriction channel at higher transit velocity than a hard one.

^a Department of Mechanical Engineering, Osaka University the Graduate School of Engineering, Suita, Japan. Fax: +81-6-6879-4185; Tel: +81-6-6879-7333; E-mail: tsai@hh.mech.eng.osaka-u.ac.jp

^b Department of Micro-Nano Systems Engineering, Nagoya University the Graduate School of Engineering, Nagoya, Japan.

^c Department of Cardiovascular Medicine, Osaka University the Graduate School of Medicine, Suita, Japan.

When evaluating cell deformability using a constriction channel, cell position, or flow-in angle, before entering the constriction channel could affect the transit velocity of the cell, and would interfere with the evaluation results. However, in the conventional design as shown in Fig. 1(a), the cells are distributed all over the cross-section before entering the evaluation channel, and it very possibly lead to a wide distribution of transit velocities as the expected results on the right of Fig. 1(a). To eliminate such kind of interference and to improve the consistency of the evaluation, a design that consists of two microchannels is proposed as shown in Fig. 1(b). When RBCs pass through the first constriction channel, they are aligned along the central region due to the laminar flow and the geometrical constraints of the channel. After leaving the alignment channel, these RBCs will stay aligned, and will be evaluated by the second constriction channel. The distribution of measured transit velocities with alignment is expected to be more concentrated, and the negative correlation between the velocity and cell size should be clearer as expected results on the right of Fig. 1(b).

The experimental study in this paper includes two parts. Firstly, RBCs from donors are evaluated with and without the alignment channel for verifying the effectiveness of the proposed method. RBC motion through the evaluation channels are captured by a high-speed camera, and cell size, position and velocity are extracted from the recorded videos using image processing. According to the obtained RBC trajectories and velocity profiles, the RBCs are effectively aligned, and the evaluation results are also found significantly improved in terms of the increasing of correlation between cell size and transit velocity. The second part of the experimental study is on the RBCs from a patient with multiple myeloma (MM) and two healthy subjects as control. An atomic force microscope (AFM), the current gold standard in cell stiffness measurement, is utilized for measuring the RBCs stiffness for the comparison with the proposed microchannel method. The results from both the AFM and proposed method show that the RBC deformability of the MM subject is widely distributed with large population of stiffened RBCs while the RBC deformability of healthy subjects are less distributed with few stiffened RBCs.

The rest of this paper is organized as follows. After a brief review on the methods of evaluation and alignment in Sec. 2, the experimental method are described in Sec. 3, which is followed by the results and discussions in Sec. 4. The case study on MM is presented in Sec. 5. Finally, the paper is concluded in Sec. 6.

2 Related Works

Different approaches of microfluidic system have been developed for evaluating cell deformability, and they can be cate-

gorized into two groups by how the cell is deformed. One of them is to deform cells by the geometrical constraint of a constriction channel. For example, Zheng *et al.* proposed a microfluidic system for high-throughput measurement which can measure 100-150 cells in one second.⁶ Chen *et al.* utilize microfluidic channel for mechanical and electrical measurement on single cells.⁷ Hirose *et al.* evaluate cell stiffness on in a microchannel for high-speed cell sorter.⁸ Tsai *et al.* proposed a dimensionless index for cell deformability using a constriction channel.⁵ The other group in microfluidic approach is to deform cells by fluid shear stress. For example, Gossett *et al.* use hydrodynamic stretching in a microfluidic system for large population mechanical phenotyping, and the evaluation rate is up to 2,000 cells per second.⁹ Katsumoto *et al.* classify single RBC deformability in high-shear microchannel flows.¹⁰ Beech *et al.* sort cell size, shape and deformability by utilizing deterministic lateral displacement.¹¹ The greatest advantages of microfluidic approach is that it has the capability of evaluating single cells at much greater throughput than direct methods, such as AFM and optical tweezers.

On the other hand, cell alignment methods have been previously developed by different techniques, such as sheath flow, optical force focusing and cell inertia.¹² Sheath flow, also known as hydrodynamic focusing, is often used for cell alignment in Lab-on-chip applications.¹³ The basic idea of the Sheath flow is to align cells by merging separated flows into a main one. The main flow will then have layers, and the flow that carries target specimen/cell is usually at the center layer. Cell alignment can also be done by manipulating cells using optical forces.¹⁴ Although both sheath flow and optical force can effectively align cells in a microfluidic channel, accurate control for the alignment is needed. Recently, the inertia of cells in a microchannel has also been used for cell alignment. For example, Di Carlo *et al.* utilized the inertial effect inside a microchannel for continuous focusing.¹⁵ The method requires no complex control but simply by geometrical design of the microfluidic device. The problem is that cell inertia is only applicable under the condition when Reynolds number is large, which means it is not suitable for evaluation with a constriction channel.

To sum up, the proposed alignment method can improve the cell evaluation in a constriction channel while requiring no additional control. To the best of the authors' knowledge, the idea of aligning cells by geometric constraints and the integration of such alignment method in a deformability evaluation system with a constriction channel are firstly proposed in this work.

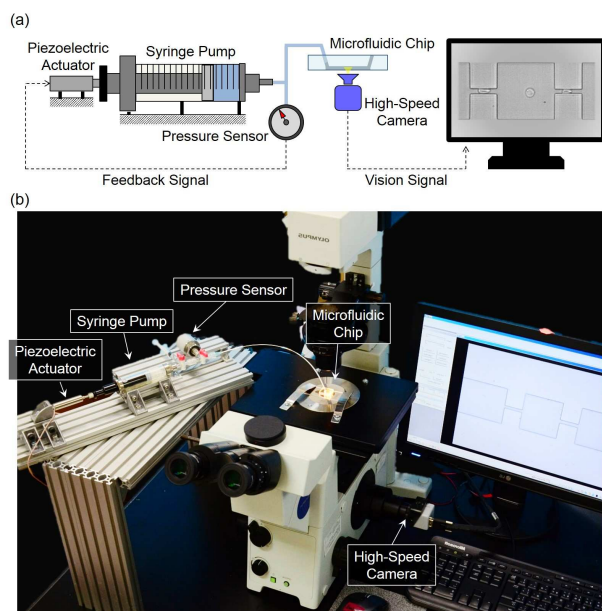


Fig. 2 (a) The overview of the experimental setup. (b) A photo of the system.

3 Method

3.1 Experimental System

Figures 2(a) and (b) shows the overview of the experimental system, and its photo, respectively. The system is constructed by three main parts including (1) a feedback pressure control system actuated by a piezoelectric actuator; (2) the proposed channel design fabricated in a Polydimethylsiloxane (PDMS) microfluidic chip; and (3) a high-speed camera for recording cell motion. The pressure control system includes a pressure sensor (FP101A, COPAL ELECTRONICS Inc.), a piezoelectric actuator (PSt150, Syouei System Co., Ltd.), a glass syringe (SGE Corp.) and a computer-based controller. The pressure control system is directly connected to the inlet of the microfluidic channel as shown in Fig.2 while the outlet is open to the atmosphere which is assumed constant during the test. The pressure difference between the inlet and outlet is kept constant during the test. The high-speed camera (IDP, PHOTRON Inc.) is mounted on the microscope (IX71, OLYMPUS Corp.) for capturing cell motion inside the microfluidic chip. The capture rate is set at 3000 frame per second (fps) while the shutter speed is set at 1/20000 second. The spatial resolution of each captured frame is 512×256 pixels, and one pixel is equivalent to the distance of $0.24 \mu\text{m}$.

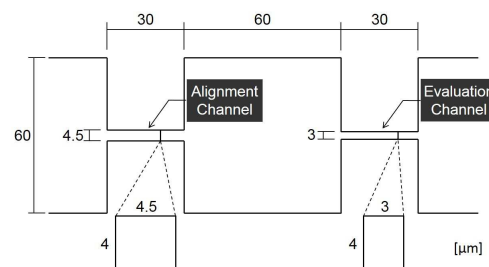


Fig. 3 The dimensions of the microfluidic channel used for the evaluation. The $4.5 \mu\text{m}$ and $3 \mu\text{m}$ channels are for RBC alignment and evaluation, respectively. The height of the channel is $4 \mu\text{m}$.

3.2 The Design and Fabrication of Microfluidic Channel

Figure 3 shows the dimensions of the proposed microfluidic design. There are two constriction channels, alignment and evaluation channels, in the design, and their width are $4.5 \mu\text{m}$ and $3 \mu\text{m}$, respectively. As reported in previous study, hundreds of transit of a RBC through a $3 \mu\text{m}$ -wide channel is needed to cause permanent damage to the cell in most of cases.¹⁶ Thus, it is fair to assume that RBCs' properties are not significantly changed by passing through the $4.5 \mu\text{m}$ -wide alignment channel before being evaluated in the $3 \mu\text{m}$ -wide evaluation channel. The PDMS microfluidic channels are fabricated from a master mold, which is made by standard photolithography procedure on a photoresist-coated (SU8-3005, MicroChem Corp.) silicon wafer. The thickness of the mold is $4 \mu\text{m}$, and is the same as the height of the fabricated channels.

3.3 Experiment Procedure

Blood samples are from volunteer donors. All the subjects, three healthy subjects and a patient with MM, have read and agreed the consent of the experiment. The blood is withdrawn by a licensed physician in a hospital. The blood is diluted with standard saline (OTSUKA Corp.) at the blood-to-saline ratio of 1 : 50 for evaluation. * The prepared sample is placed on a shaker for 10 minutes for RBCs to adapt to the saline environment. In the meantime, the saline solution is injected into the PDMS channel, so the surface inside the microfluidic channel is wetted, and the environment in the channel is similar to the prepared sample.

Finally, the prepared RBC samples are injected into the channel from the inlet of the microfluidic chip, and then the constant-pressure pump is connected to the inlet to establish a constant flow. RBCs are carried by the flow moving from the

* There are about 5 million RBCs in $1 \mu\text{l}$ of whole blood. Dilution is necessary for observing single cell behavior through a microfluidic channel.

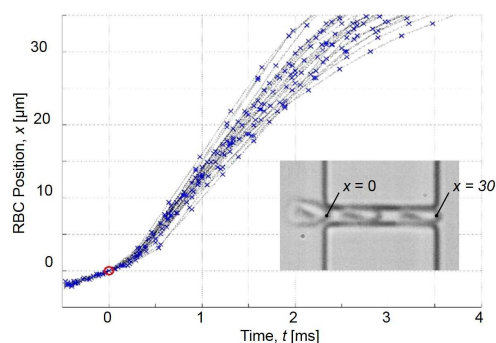


Fig. 4 Examples of tracked RBC motion in the experiment.

inlet to outlet, and the behavior through the evaluation channel is recorded by the high-speed camera. The experiment is performed in the room temperature at 25 °C. The pressure difference between the inlet and outlet of the channel is kept at 4 kPa. The pressure variation during the test is controlled within 0.1 kPa according to the measured pressure, thus the flow condition inside the channel is considered as constant.

Blood cells other than RBCs have been seen in the microchannel during a test[†]. For the cells smaller than RBC, such as platelets, they usually have no problem passing through the constrictions, and can be easily distinguished in the analysis by cell size. On the other hand, for the bigger ones, such as white blood cells (WBCs), they often clog the constrictions because of the large size. For the clog that can be removed by the flow, the recorded data before and after the clog will be given up due to the possible inconsistent flow caused by the clog. In the situation that the clog cannot be simply removed by the flow, the clogged PDMS chip will be replaced by a new one.

3.4 Motion Analysis and Deformability Evaluation

3.4.1 Cell Tracking by Image Processing

RBCs' size and trajectories are extracted from the recorded videos by cell tracking program developed in Matlab (Mathworks Corp.), and the velocity of each RBC is calculated from its moving trajectory with respect to time. RBCs sometimes have flipping motion inside the microchannel, which may affect the cell evaluation.¹⁸ Since the flipping motion corresponds to significant size change from the top view through the microscope, it can be automatically detected by the program. However, the flipping motion inside the constrictions cannot be clearly judged due to the limited dimensions and resolution of acquired images. To compensate it and to assure the validity of the evaluation, the cell motion which is

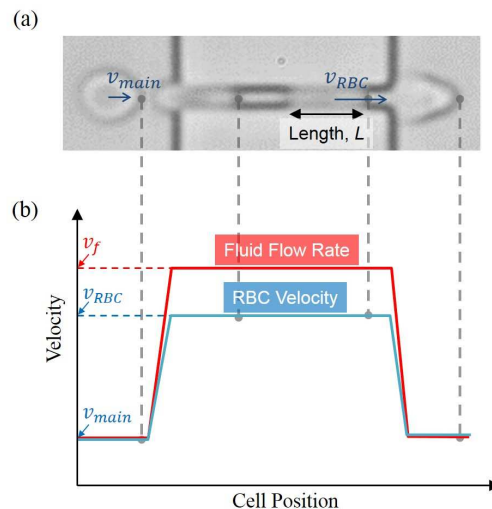


Fig. 5 The relation between RBC transit velocity, v_{RBC} , and fluid velocity, v_f , inside the evaluation channel. The transit velocity is normalized by fluid velocity using Eq.(1) for representing the cell deformability.

different from others will be visually examined, and will be removed from the evaluation result if the flipping motion is found.

Figure 4 shows an example of tracked results plotted on a time-position plane. The origin ($t = 0$ [ms] and $x = 0$ [μm]) on the plot is defined as the moment and cell position when a RBC is at the entrance of the evaluation channel. The cell length, L , in the channel is measured as an index of cell size, and RBC transit time in the given pressure is ranged from 2 to 4 [ms] as shown in Fig. 4. By considering the average transit time of 4 [ms] and the condition of RBCs being continuously fed into the evaluation channel, the system is capable of evaluating single-cell deformability up to 250 cells per second[‡].

3.4.2 Cell Deformability Index Although the pressure difference between the inlet and outlet of the microfluidic channel is maintained constant, slight difference in the flow from one test to another is still possible due to different RBC numbers and flow resistance between different microfluidic chips. To compensate such difference, the normalized transit velocity, \hat{v} , of each cell is utilized as the index of RBC deformability, and is defined as

$$\hat{v} = \frac{v_{RBC}}{v_f} \quad (1)$$

where v_{RBC} and v_f are the measured cell transit velocity and the estimated velocity of fluid flow inside the evaluation chan-

[†] The chance of observing other cells is relatively low since the ratio of RBCs, white blood cells and platelets of normal human blood is 1000:1:40¹⁷

[‡] A proper cell sorting system to continuously feed cells into the evaluation channels is needed in order to achieve such a high throughput.

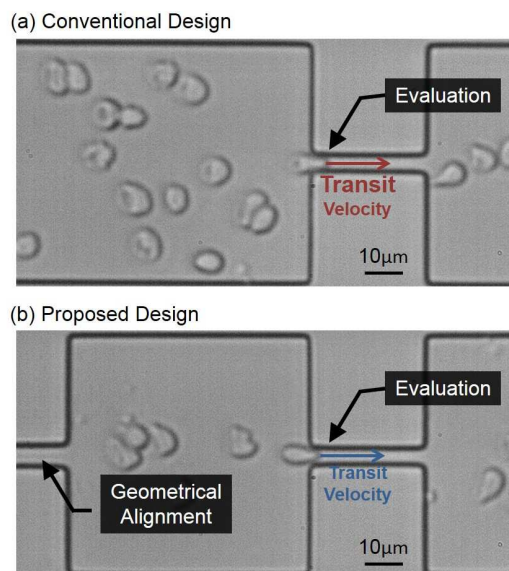


Fig. 6 The snapshots from the experimental videos. (a) without alignment channel. (b) with alignment channel.

nel, respectively. The transit velocity, v_{RBC} , is the average velocity of a RBC passing through the constriction channel, and is calculated based on the first and last tracked points of the RBC within the evaluation channel. The estimated fluid velocity, v_f , is calculated based on the RBC velocity in the main channel[§], and the ratio between the width of the main channel and the evaluation channel, which is

$$v_f = v_{main} \frac{w_{main}}{w_{eva}} \quad (2)$$

where v_{main} , w_{main} and w_{eva} are the measured RBC velocity in the main channel, the width of the main channel the evaluation channel, respectively. Since individual RBC velocity in the main channel may differ from one to another due to different position on a cross-section, the average value of the cell velocities in the main channel among all detected RBCs is calculated for v_{main} in the evaluation.

Figure 5 illustrates the relation between fluid velocity and RBC transit velocity represented in red and blue lines, respectively. The two lines are overlapped before RBCs reaching the constriction channel because cell velocity is assumed the same as the fluid velocity due to low Reynolds number. While RBCs are squeezing into the channel whose width is only $3 \mu\text{m}$, the cells are greatly deformed, and result in significant resisting force against cells moving forward. As a result, the velocity of the cell becomes less than the fluid velocity, which leads to

$$v_{RBC} < v_f \implies \hat{v} < 1 \quad (3)$$

[§] v_{main} is the average velocity of a RBC when its position, x is $-40 < x < -20$ [μm]. $x = 0$ is defined as the entrance of evaluation channel as in Fig. 4

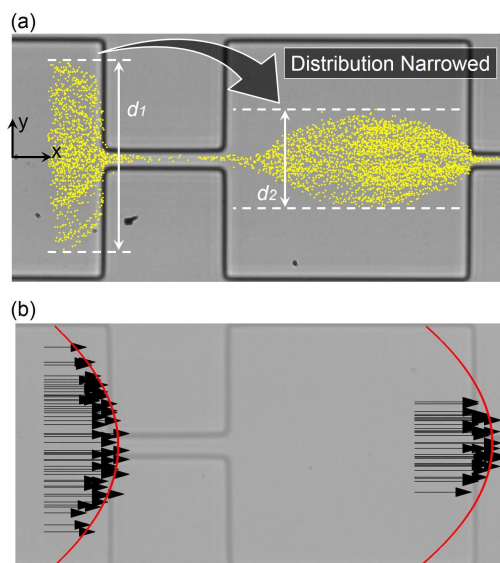


Fig. 7 (a) The trajectories of RBCs flow through two constriction channels. (b) The velocities of RBCs with respect to their positions. The red curves are the fitting results representing the velocity profiles.

If a RBC is extremely small compared with the width of the evaluation channel, there will be no deformation, and the velocity of the cell would be the same as it of the fluid. The normalized velocity of the RBC becomes

$$\hat{v} = 1 \quad (4)$$

After the normalization using Eq. (1), a RBC is said to have high deformability if its \hat{v} is close to 1. The deformability is said to be low when the \hat{v} is close to 0.

4 Experimental Results

4.1 Effectiveness of Cell Alignment

Figures 6(a) and (b) show snapshots of experiments without and with alignment channel, respectively. The positions of RBCs without the alignment channel are distributed along the vertical direction while the distribution of RBCs' positions with the alignment channel is clearly suppressed. Figure 7 shows the effectiveness of cell alignment based on a tracking result. In Fig. 7(a), each yellow dot represents a tracked point of a RBC in a video frame, and all points together show the trajectories of RBCs flowing, from left to right, inside the channel. The distribution of RBC position along y axis, perpendicular to the flow direction, is notably better focused after passing through the alignment channel. The width of the distribution is measured as the distance from the top to the bottom

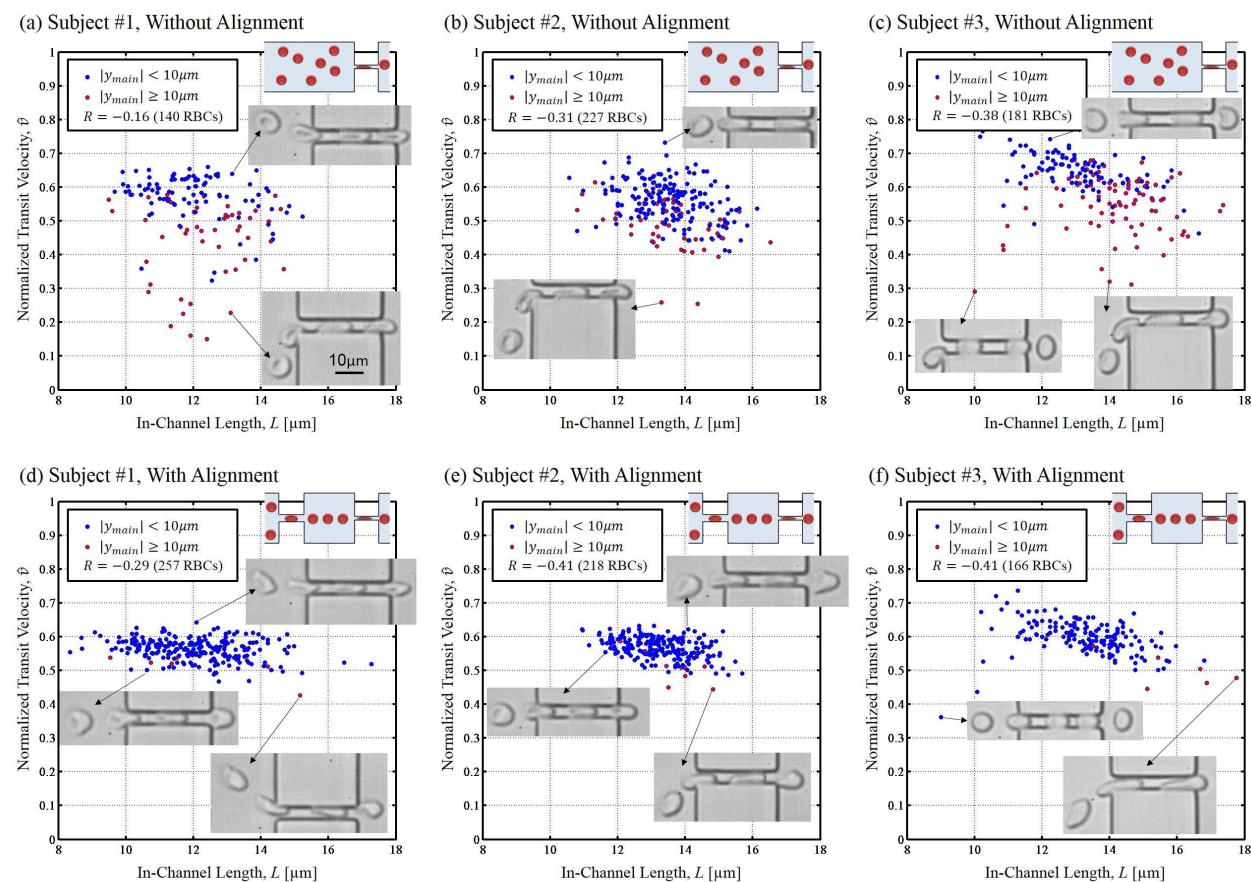


Fig. 8 The evaluation results of three healthy subjects. (a)-(c) show the results without alignment, and (d)-(f) show the results with alignment. The pairs of (a)(d), (b)(e) and (c)(f) are the results from the same subjects. In (a)-(f), the blue and red data points indicate the RBC flow into the constriction channel along the central region and outside the central region, respectively. Examples of RBCs images are included in each plot.

Table 1 Effectiveness of Alignment by Distribution Width d_1 and d_2

| | d_1 [μm] | d_2 [μm] | Δd [%] |
|---------|-------------------------|-------------------------|----------------|
| Test #1 | 46.8 | 27.8 | 40.5% |
| Test #2 | 45.8 | 26.2 | 42.9% |
| Test #3 | 46.3 | 25.7 | 44.6% |

of all tracked points. The distribution widths before and after the alignment channel are indicated as d_1 and d_2 as shown in the Fig. 7(a). The measured d_1 , d_2 and the percentage of reduction, $(d_1 - d_2)/d_1$, from the results are tabulated in Table 1.

Figure 7(b) shows the cell velocities before and after the alignment channels. The x components of RBCs' velocities are shown in black arrows. The arrows' roots, directions and lengths indicate the cell position where the velocities are mea-

sured, the direction and the magnitude of velocities, respectively. The red curves are the velocity profiles obtained by curve fitting on the velocities with respect to the positions on y-axis. From the results in Fig. 7, it can be visually observed that the variations of both the positions and velocities of RBCs are significantly reduced after the alignment channel.

4.2 Evaluation With/Without Alignment

Figure 8 shows experimental results with and without the proposed alignment channel on the RBCs from three healthy subjects. The data points are extracted from videos captured during the test, and the total recording time is less than 15 seconds for each RBC sample. After removing the results of the cells other than RBCs and also the results where more than one RBCs inside the constriction at the same time, more than 140 RBCs are successfully tracked for each test. Figures 8(a)-(c)

are the results without alignment channel, while Figs. 8(d)-(f) show the results with alignment channels with the same RBCs corresponding to (a)-(c). The x and y axes in Figs. 8(a) to (f) are the cell length in the channel and deformability index by Eq.(1). The plots are expected to be negatively correlated because a larger RBC is likely to have greater in-channel length, L , and less normalized velocity, \hat{v} . The blue and red points in Fig. 8 indicate the RBCs flow into the constriction channel along the central region and outside the central region, respectively. The vertical position of each RBC in the main channel is represented by y_{main} , which is obtained from its trajectory. When $y_{main} = 0$, it means the RBC moves along the center line in the main channel.

Two observations can be seen from the distribution of the data points in Fig. 8. First, the tendency of RBCs response from different flow-in position is clearly different that the ones flow into the channel outside the central region ($|y_{main}| \geq 10$) are consistently having lower transit velocities as the red points indicated in Fig. 8. The ones flow inside the central region ($|y_{main}| < 10$) show better correlation between \hat{v} and L . The second observation is that the RBCs along the central region in Fig. 8(a)-(c) are located in similar locations as the ones in Fig. 8(d)-(f). This result supports that the proposed alignment improves the evaluation by removing the cell flow into the constriction outside the central region. While RBCs enter the channel outside the central region, RBCs are bent due to the dramatic change of moving direction, and almost "hang" on the edge of the entrance as the RBC images associated with red points shown in Fig. 8. Such sharp turn significantly slows down RBCs' velocities while entering the constriction, and consequently, reduces transit velocity of the RBCs. Since such low \hat{v} is due to cell motion but not cell property, it is not desirable for the evaluation. The negative correlation, R , between the length and deformability is improved from the results without alignment to the results with alignment. The negative correlation can be interpreted as that cell deformability reduces with cell size increases, which makes physical sense that a large cell moves slower in the constriction than a small one due to greater amount of deformation if the same cell deformability is assumed.

There are exceptions away from the majority population of the data points where the RBCs show low \hat{v} in Fig. 8. Those RBCs are visually examined, and are found having different deformability from other RBCs. An example is shown in Fig. 8(f) at $(L, \hat{v}) = (9.0, 0.36)$. Such exceptions show that the proposed method can perform a scan of large population of RBCs for finding the RBC with specially low deformability while obtaining the cell deformability of majority population.

The experimental conditions, such as how the velocity is calculated, the width of the constriction, the flow rate inside the microchannel and the type of suspension solution, can also affected the results of evaluation. Therefore, the experimental

results by different conditions are presented in Appendix I for further information to the microfluidic evaluation.

5 Evaluation on Multiple Myeloma RBCs

Multiple Myeloma is a type of cancer in which normal blood cells cannot be produced from bone marrow due to abnormal plasma cells. There are two aims in this experimental study. The first aim is to validate the proposed microfluidic evaluation approach by comparing it with the results from AFM, the current gold standard method of cell stiffness measurement. Although the RBC stiffness and transit velocity are not exactly the same in terms of unit and physical meaning, but they both reflect the deformability of RBCs. Therefore, it is expected to see the same tendency of the RBCs' deformability from both of them. For example, a RBC with relatively low transit velocity should have relatively high stiffness from AFM since low transit velocity reflects low cell deformability. The second aim is to see how if there is any significant difference between the RBC deformability from the patient with MM to the healthy subjects.

The patient's RBCs are evaluated along with the RBCs from two other healthy subjects. The evaluation channel with the width of $2\mu\text{m}$ is utilized for the test, and the Dulbecco's PBS (D8537, Sigma Corp.) is used for RBC dilution and suspension. On the other hand, an AFM (Nanocute SII, HITACHI Corp.) is employed for measuring RBC stiffness under three different indentation depths, 100, 200 and 300 nm.

Figure 9 summarizes the evaluation results of the test, and the columns from left to right are the results of the patient and two healthy subjects, respectively. Figures 9(a)-(c) are the results of AFM measurement while (d)-(f) are the results of the proposed method.[¶] Figure 9(g)-(i) are the measured diameter of undeformed RBCs in the microchannel before entering the channel. According to the results in Figs. 9(a)-(c), the RBC stiffness of MM patient are varied from 4 to 33 [kPa] while the RBC stiffness of two other healthy subjects are constantly under 15 [kPa]. The similar tendency are observed by the proposed method in Figs. 9(d)-(f) that the data of the MM patient is more scattered in Fig. 9(d) than the healthy subjects in Figs. 9(e) and (f). The Fig. 9(g)-(i) shows that all three subjects having similar size distribution of RBCs, so the scattering of the cell stiffness/deformability of MM subject may not due to the RBC size but RBC deformability.

In order to reduce the possible effect from time and keep the both evaluations within the similar time period as the time from blood withdrawal, only very limited RBC samples are obtained in AFM measurement. It is due to the nature of AFM measurement which takes several seconds, or even minutes, to

[¶] the large RBCs ($L > 20[\mu\text{m}]$) are removed after visual examination for avoiding the case of rouleaux formation which has been previously reported as a symptom of MM.¹⁹

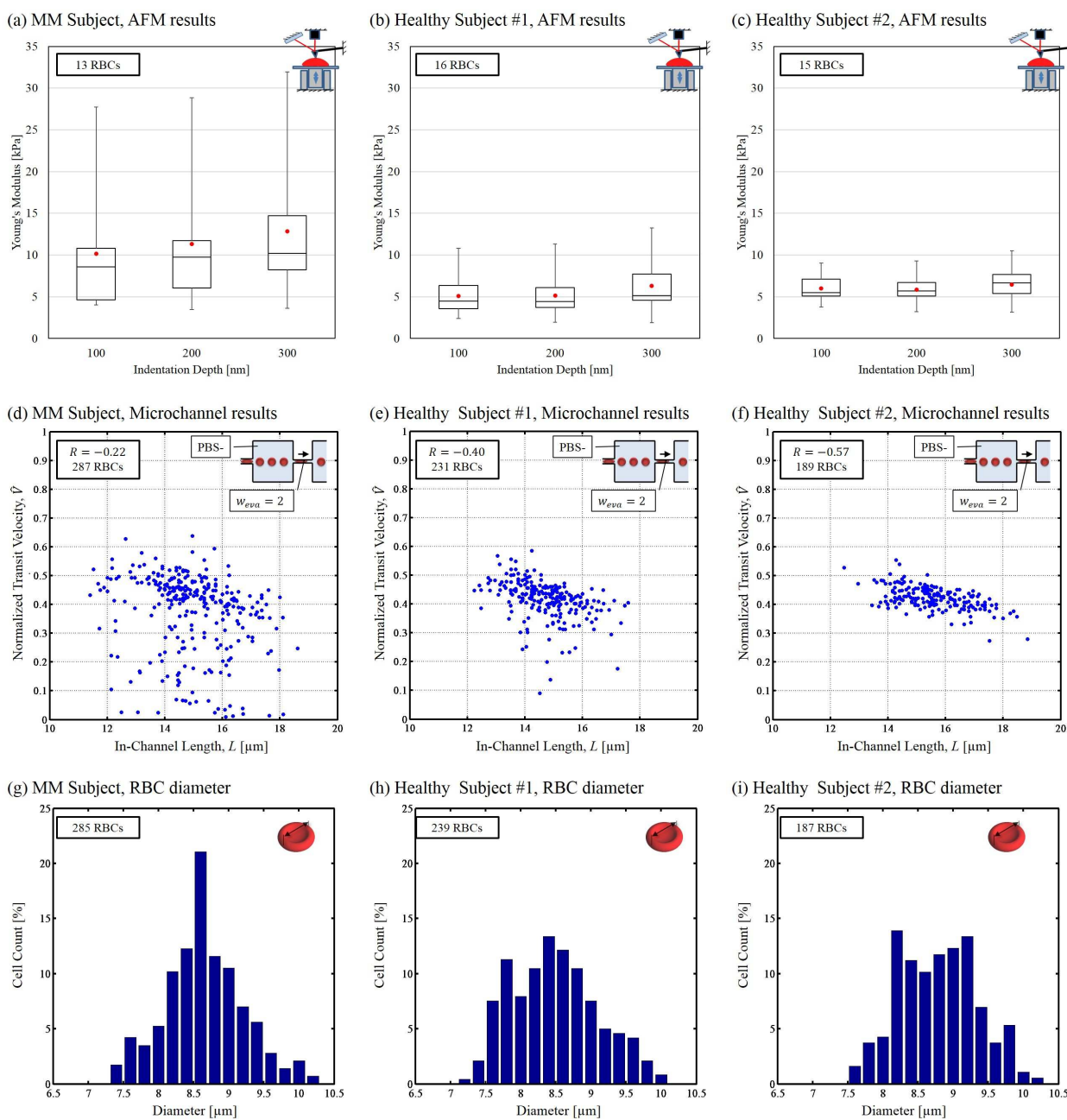


Fig. 9 The comparison between MM subject (1st column) and two healthy subjects (2nd and 3rd columns). (a)-(c) RBC stiffness measured by AFM. (d)-(f) The relation between RBC transit velocity and in-channel length corresponding to Figs. 9(a)-(c). (g)-(i) The distribution of RBC diameter, corresponding to Figs. 9(a)-(c), measured inside the microfluidic channel before entering the constrictions.

measure one RBC. On the other hand, the experimental time in the proposed method for each blood sample is about 15 seconds, not including the sample preparation and image processing, but hundreds of RBCs behavior can be recorded by the vision system. This again shows the great advantage of high-throughput of the microfluidic approach in cell evaluation.

6 Conclusion

A microfluidic design with geometrical alignment for improving the sensitivity of evaluating cell deformability is proposed and tested. Four concluding remarks are:

1. The proposed microfluidic design provides a simple and effective method for cell alignment in the evaluation of cell deformability. Cells are spontaneously aligned by the geometrical constraints without any additional control.
2. The sensitivity to cell size is clearly enhanced by the proposed alignment from conventional microchannel approach. The correlation between cell size and transit velocity increases with cell alignment compared with the ones without cell alignment under the same conditions.
3. RBC deformability evaluated by the proposed method is compared with the RBC stiffness measured by an AFM, the current gold standard in cell stiffness measurement. The comparison shows the similar tendency between two methods, which supports the validity of the proposed method.
4. The patient with MM is found having large population of stiffened RBCs while only few stiffened RBCs are detected from the RBCs of healthy subjects.

Acknowledgement

We would like to thank Mr. Shuhei Yoshikawa and Mr. Kohei Ochi for their assistance in the experiments. This work is supported by Grant#23106003 and #26820086 of The Ministry of Education, Culture, Sports, Science and Technology (MEXT) of Japan.

Appendix A

Effect of Experimental Conditions

Figure 10 shows the results of the RBCs from the same source evaluated under five difference combinations of experimental conditions. Figure 10(a) illustrates the conditions, and Fig. 10(b) is the control group for the other four results in Figs.10(c)-(f). The five difference conditions are varied in three condition categories, and the details are as follows:

1. **The way of calculating normalized transit velocity \hat{v} .** Figure 10(b) and (c) shows including and excluding the phase of cell deformation, respectively. It shows the transit velocities are increase by excluding the phase of deformation. In other words, the transit velocity of each RBC in Fig. 10(b) is calculated as the average velocity from RBC just reaches the channel entrance until the RBC reaches the channel exit while the transit velocity is calculated from the RBC fully entering the channel While the advantage is that RBC entering position no longer affect the cell evaluation, the disadvantage is that we lose the information of cell transient response during deformation. In the case that the overall cell deformability is considered, the transit velocity including deformation phase should be utilized.
2. **The flow rate inside the microchannel.** The flow rate is represented by the RBC transit velocity, and Fig. 10(b) and (d) shows the cases of $v_{RBC} = 7 \pm 2[\mu m/ms]$ and $0.7 \pm 0.2[\mu m/ms]$, respectively. It is interesting to see that even with 10 times difference in the transit velocity, the two sets of data are largely overlapped in the plot, and the difference is that the in-channel length in the slower flow rate is slightly shifted to the left. This shows that the normalization method in Eq.(1) effectively compensate the effect coming from the different flow condition, and similar results can be obtained under the transit velocity within these ranges.
3. **The selection of solution for RBC suspension and dilution.** Three different solutions commonly used in biology experiment, standard saline, phosphate-buffered saline without magnesium and calcium (PBS-) and phosphate-buffered saline with magnesium and calcium (PBS+), are tested, and the results are in Figs. 10(b), (e) and (f), respectively. There is no significant difference between these three solutions in this condition test, especially with standard saline and PBS-. The \hat{v} in PBS+ is found slightly increased and the width of L distribution is reduced.

References

- 1 F. K. Glenister, R. L. Coppel, A. F. Cowman, N. Mohandas and B. M. Cooke, *Blood*, 2002, **99**, 1060–1063.
- 2 H. Bow, I. V. Pivkin, M. Diez-Silva, S. J. Goldfless, M. Dao, S. S. J. C. Niles and J. Han, *Lab on a Chip*, 2011, **11**, 1065–1073.
- 3 M. Brandao, A. Fontes, M. Barjas-Castro, L. Barbosa, F. Costa, C. Cesar and S. Saad, *Eur. J. Hematol*, 2003, **70**, 207–211.
- 4 K. Tsukada, E. Sekizuka, C. Oshio and H. Minamitani, *Microvascular Research*, 2001, **61**, 231–239.
- 5 C. D. Tsai, S. Sakuma, F. Arai and M. Kaneko, *IEEE Transactions on Biomedical Engineering*, 2014, **61**, 1187–1195.
- 6 Y. Zheng, E. Shojaei-Baghini, A. Azad, C. Wang and Y. Sun, *Lab on a Chip*, 2012, **12**, 2560–2567.

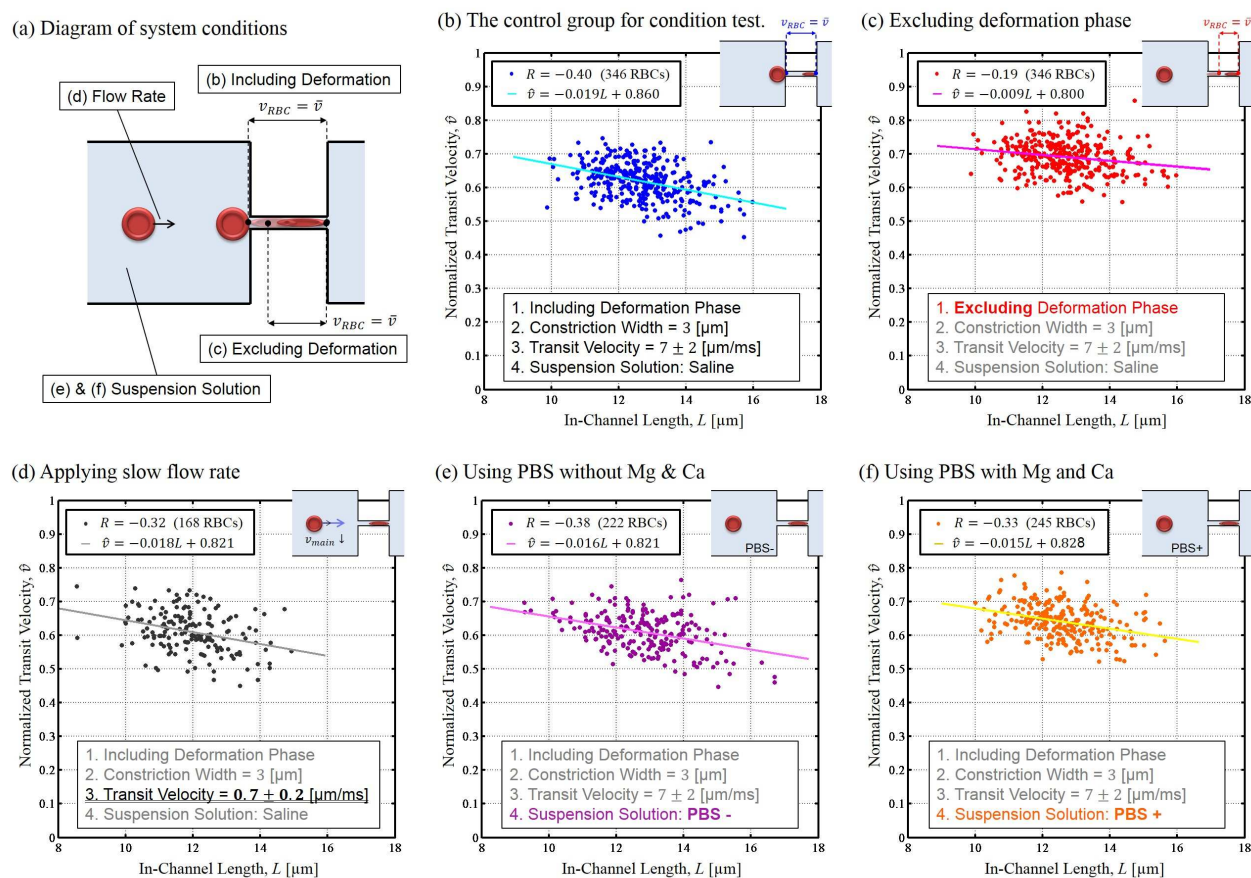


Fig. 10 The experimental results on RBC evaluation under different conditions. (a) The diagram showing the tested conditions; (b) The condition where deformation phase is included for RBC transit velocity; (c) The condition where deformation phase is excluded for RBC transit velocity; (d) The condition where 1/10 times flow rate is applied during the test; (e) The condition where PBS- is used for RBC suspension and dilution; (f) The condition where PBS+ is used for RBC suspension and dilution.

- J. Chen, Y. Zheng, Q. Tan, E. Shojaei-Baghini, Y. L. Zhang, J. Li, P. Prasad, L. You, X. Y. Wu and Y. Sun, *Lab On A Chip*, 2011, **11**, 3174–3181.
- Y. Hirose, K. Tadakuma, M. Higashimori, T. Arai, M. Kaneko, R. Iitsuka, Y. Yamanishi and F. Arai, Proc. of the IEEE Int. Conf. on Robotics and Automation, ICRA, Anchorage, USA, 2010, pp. 4113–4118.
- D. R. Gossett, H. T. K. Tse, S. A. Lee, Y. Ying, A. G. Lindgren, O. O. Yang, J. Rao, A. T. Clark and D. D. Carlo, Proc. of the National Academy of Sciences, PNAS, 2012, pp. 7630–7635.
- Y. Katsumoto, K. Tatsumi, T. Doi and K. Nakabe, *Int. J. Heat Fluid Flow*, 2010, **31**, 985–995.
- J. P. Beech, S. H. Holm, K. Adolffson and J. O. Tegenfeldt, *Lab on a Chip*, 2012, **12**, 1048–1051.
- Y. Zheng, J. Nguyen, Y. Wei and Y. Sun, *Lab on a chip*, 2013, **13**, 2464–2483.
- B. Zhao, J. S. Moore and D. J. Beebe, *Science*, 2001, **291**, 1023–1026.
- K. B. Roth, C. D. Eggleton, K. B. Neeves and D. W. M. Marr, *Lab on a Chip*, 2013, **13**, 1571–1577.
- D. D. Carlo, D. Irimia, R. G. Tompkins and M. Toner, Proc. of the National Academy of Sciences, PNAS, 2007, **104**, 18892–18897.
- S. Sakuma, K. Kuroda, C. D. Tsai, W. Fukui, F. Arai and M. Kaneko, *Lab On A Chip*, 2014, **14**, 1135–1141.
- J. Greer, D. Arber, B. Glader, A. List, R. Means, F. Paraskevas, G. Rodgers and J. Foerster, *Wintrobe's Clinical Hematology 12th Edition*, LWW, 2013.
- J. Wan, A. M. Forsyth and H. A. Stone, *Integrative Biology*, 2011, **3**, 972–981.
- M. Dimopoulos and R. K. et al., *Blood*, 2011, **117**, 4701–4705.